frontiers | Frontiers in Earth Science

ORIGINAL RESEARCH
published: 05 July 2022
doi: 10.3389/feart.2022.927876

Interdecadal Variability of Spring Eurasian Snowmelt and Its Impact on Eastern China Summer Precipitation

Fei Cheng[1], Qiaoping Li[2], Jing Wang[3], Yanju Liu[4], Yihui Ding[4], Xinyong Shen[1,5] and Chengyu Song[1]*

[1]Key Laboratory of Meteorological Disaster, Ministry of Education/Joint International Research Laboratory of Climate and Environment Change/Collaborative Innovation Center on Forecast and Evaluation of Meteorological Disasters, Nanjing University of Information Science and Technology, Nanjing, China, [2]CMA Earth System Modeling and Prediction Centre (CEMC), China Meteorological Administration, Beijing, China, [3]Tianjin Key Laboratory for Oceanic Meteorology, Tianjin Institute of Meteorological Science, Tianjin, China, [4]National Climate Center, China Meteorological Administration, Beijing, China, [5]Southern Marine Science and Engineering Guangdong Laboratory (Zhuhai), Zhuhai, China

In this study, the interdecadal variability of Eurasian spring snowmelt and its relationship with Eastern China summer precipitation (ECSP) are investigated based on observations and reanalysis data. Results show that the second mode of the empirical orthogonal function (EOF) analysis of the spring snowmelt, featured as a west-east dipole pattern, displays two interdecadal changes near the late-1970s and in the mid-2000s. The increased spring snowmelt over the Western Siberia (WSI) and the opposite situation over the Eastern Europe (EEU) are significantly linked to a meridional quadrupole summertime rainfall pattern on interdecadal time scales, with excessive rainfall over the regions of southern China (SC) and the Huang-Huai River (HHR) and deficient rainfall over the middle and lower reaches of Yangtze River Valley (YRV) and Inner Mongolia-northeastern China (IMNC). Besides, the possible mechanisms are discussed from the perspective of the hydrological effect related to snowmelt-induced soil moisture. Increased spring snowmelt can produce more water inflowing into the soil, leading to anomalous soil moisture, which can persist into summer. Excessive (deficient) snowmelt-related soil moisture anomalies over the WSI (EEU) in summer will change local land thermal conditions and thus generate cyclonic (anticyclonic) circulations with a quasi-barotropic structure. Therefore, the eastward-propagating wave-activity flux (WAF) could be strengthened over the WSI and EEU in the mid- and upper-troposphere and further propagate downstream. Combining the local response of atmospheric circulations to summer surface heating induced by local snowmelt-related SM anomalies over Mongolia, an anomalous anticyclonic (cyclonic) circulation near the Lake Baikal (SC) and the related strong descending (ascending) motion over the IMNC (SC) are founded. Besides, strong positive (negative) upper-level divergence appears over the YRV (HHR), which is the right (left) side of the exit region of upper-level jet. The upper-level divergence could be attributed to the convergence (divergence) of meridional winds on the right side of the anticyclonic circulation, thus the uniform descending (ascending) motion also appears over the YRV (HHR) through the collocation of upper-level convergence (divergence) and the compensatory lower-level circulations. Consequently, a quadrupole pattern of

OPEN ACCESS

Edited by:
Jianqi Sun, Institute of Atmospheric Physics (CAS), China

Reviewed by:
Chenghai Wang, Lanzhou University, China
Huopo Chen, Institute of Atmospheric Physics (CAS), China

***Correspondence:**
Qiaoping Li
liqp@cma.gov.cn

Specialty section:
This article was submitted to Atmospheric Science, a section of the journal Frontiers in Earth Science

Received: *25 April 2022*
Accepted: *13 June 2022*
Published: *05 July 2022*

Citation:
Cheng F, Li Q, Wang J, Liu Y, Ding Y, Shen X and Song C (2022) Interdecadal Variability of Spring Eurasian Snowmelt and Its Impact on Eastern China Summer Precipitation. Front. Earth Sci. 10:927876. doi: 10.3389/feart.2022.927876

secondary circulation over Eastern China is founded, thereby causing the anomalously distributed ECSP under favorable water vapor conditions.

Keywords: spring snowmelt, eastern china summer precipitation, interdecadal variation, soil moisture, atmosphere-land interaction

1 INTRODUCTION

Snow cover has high reflectivity, high emissivity and low thermal conductivity. It has a significant impact on local climate by changing surface radiation, water budget and hydrological cycle, and further influences the downstream and even global climate through teleconnection (Barnett et al., 1989; Yasunari et al., 1991; Essery, 1997; Xu et al., 2012).

Eurasian snow cover in winter and spring, which accounts for 60 percent of the whole snow cover extent over the Northern Hemisphere (Robinson et al., 1993), has been long considered as a significant driving factor of the Asian summer monsoon and precipitation in China (Li and Wang, 2011; Zhang et al., 2016; Lu M. M. et al., 2020; Lu M. et al., 2020). Many previous studies have explored the linkage between Eurasian snow cover and Eastern China summer precipitation (ECSP), and revealed that the Eurasian spring snow cover contributes substantially to the subsequent East Asian summer rainfall on interannual time scales (Yang and Xu, 1994; Kripalani et al., 2002; Dash et al., 2005; Wu and Kirtman, 2007). Chen and Song (2000) found that excessive Eurasian snow cover in spring corresponds to less (more) precipitation observed in the southern (northern) part of eastern China. Liu and Yanai (2002) proposed that large Eurasian snow cover in spring leads to the cooling and cyclonic circulation anomalies in the lower layer over Eurasia, triggering a Rossby wave train and then leading to below normal EASM rainfall. Shen et al. (2020) revealed that the Siberia snow cover in late spring is closely related to the summer precipitation in south-central China. However, snow anomalies over Western Eurasia are often opposite to those over eastern Eurasia (Dash et al., 2005). Yim et al. (2010) further indicated that the East Asian summer rainfall is more closely linked to the west-east dipole mode than the uniform mode of spring snow cover anomaly over the whole Eurasian continent. These studies have revealed that the conclusions of the relationship between Eurasian spring snow cover and ECSP are often inconsistent due to the differences in study areas or methods.

As limited by the data length of snow cover used before, relatively few researches have been conducted on the interdecadal variability of Eurasian spring snow cover and its relationship with the ECSP. Zhang et al. (2008) proposed that the increase in southern China precipitation after the late 1980s may be associated with the interdecadal decrease of spring snow cover. Wu et al. (2009) revealed that the excessive Eurasian spring snow cover before the late 1980s was related to abundant rainfall in southern China and deficient rainfall in northern and northeastern China. Nevertheless, the north-south dipole pattern of ECSP only appears after the 1990s (Sun and Wang, 2015; He et al., 2017). Zhang et al. (2021) further proposed that the Eurasian spring snow cover is insignificantly (significantly) related to the ESCP before (after) the 1990s. Hence, there is no robust relationship between the Eurasian spring snow cover and the ECSP on interdecadal time scales, and the corresponding physical mechanism is not clear as well. Therefore, further research on interdecadal time scales needs to be done. Meanwhile, influenced by numerous factors, the interdecadal variability of East Asian summer monsoon precipitation is very complicated, with multiple time scales and spatial patterns (Ding et al., 2008; He et al., 2017; Zhang et al., 2018). As snow is an essential land surface forcing factor, it is also necessary to better understand the interdecadal variability of the ECSP from the perspective of preceding snow cover conditions at middle latitudes.

But how can the preceding snow cover exert its lagged impact on ECSP? The main effects of snow cover manifest as the albedo effect and the hydrological effect, with the latter being considered more important (Cohen and Rind, 1991; Gong et al., 2004). Barnett et al. (1989) pointed out that the snow-albedo effect cannot persist into summer, but the snow-hydrological effect resulting from snowmelt processes can influence the climate in next several months through soil moisture memory. The relative importance of the albedo effect over the hydrological effect varies in different latitudes and seasons, with the hydrological effect being dominant in mid-latitude areas in summer while the albedo effect leading in lower-latitude areas in spring and early summer (Yasunari et al., 1991; Souma and Wang, 2010). Xu and Dirmeyer (2013) further confirmed that the albedo effect only works before and during snowmelt processes with its dominant areas of land-atmosphere coupling shifting northward following the snow cover retreat; while the hydrological effect occurs as soon as the snowmelt starts, and it can continue to work in several months afterward. It is worth noting that previous studies were mainly based on the snow cover variability itself. However, the amount of spring snowmelt is a more direct reflection of the hydrological cycle than the snow cover itself (Sun et al., 2021). At present, a number of studies have focused on the spring snow decrement (SSD) when exploring the linkage between spring snow cover and the subsequent climate (Han et al., 2014; Sun et al., 2021; Zhou et al., 2021). For example, Zhang et al. (2017) disclosed a close relationship between the interannual variability of spring snowmelt and the East Asian summer rainfall. However, on the interdecadal time scales, less attention has been paid to the process of how the snowmelt influences the ECSP, which deserves further investigation.

This study aims to investigate the interdecadal variability of the Eurasian spring snowmelt and its impact on the ECSP, as well as the associated physical mechanisms. The remainder of this paper is organized as follows. **Section 2** describes the data and methods adopted in the present study. **Section 3** presents the interdecadal variability of the Eurasian spring snowmelt and its

relationship with the ECSP. **Section 4** explores the possible physical mechanisms. The conclusions and discussion are given in **Section 5**.

2 DATA AND METHODS

2.1 Data

The data used in this study are as follows. The monthly mean precipitation data in China with a horizontal resolution of 0.5° × 0.5° is provided by National Meteorological Information Center (NMIC) of the China Meteorological Administration (CMA), The monthly global precipitation data with a horizontal resolution of 1° × 1° is obtained from the Global Precipitation Climatology Centre (GPCC). The remaining data are derived from the fifth generation European Reanalysis (ERA5), provided by European Centre for Medium-Range Weather Forecasts (ECMWF), including the monthly gridded snow water equivalent (SWE) data and monthly mean atmospheric data with a horizontal resolution of 1° × 1°, the monthly mean soil moisture in four layers with depths of 0–7 cm, 7–28 cm, 28–100 cm and 100–289 cm, and surface heat flux data. Note that the ERA5 data before 1979 are derived from datasets of the preliminary version, which had confirmed its consistency with most other observations covering the same periods in many aspects, especially the global surface temperature and precipitation (Bell et al., 2021). The time period in this study is from 1961 to 2020, which is the common range of all datasets.

2.2 Methods

According to Sun et al. (2021) and Zhou et al. (2021), the SSD is defined as the SWE difference between March and May, with positive SSD representing snowmelt. The empirical orthogonal function (EOF) analysis is employed to capture the dominant modes of SSD variation. Additionally, the linear regression analysis is conducted to examine the relationships of the SSD with the ECP in summer as well as other relevant physical quantities. Before analysis, the long-term linear trends are removed to eliminate the climate warming effect. Here, as we mainly focus on the interdecadal time scales, a 9-years low-pass Lanczos filter (Duchon, 1979) is used to extract the interdecadal components of the raw data. Besides, the Student's *t*-test is utilized to evaluate the statistical significance of the results. Since the 9-years low-pass filtered series substantially reduce the degree of freedom of the raw data, the effective degrees of freedom N^{eff} are calculated by the following equation (Pyper and Peterman, 1998):

$$\frac{1}{N^{eff}} \approx \frac{1}{N} + \frac{2}{N}\sum_{j=1}^{N}\frac{N-j}{N}\rho_{XX}(j)\rho_{YY}(j)$$

where N is the length in time dimension; $\rho_{XX}(j)$ and $\rho_{YY}(j)$ are the j th-order autocorrelations for the time series of ρ_{XX} and ρ_{YY}, respectively.

The horizontal wave activity flux (WAF) is calculated according to Takaya and Nakamura (2001) as follows:

$$\mathrm{WAF} = \frac{p\cos\varphi}{2|\mathrm{U}|}\left\{\begin{array}{l}\frac{U}{\alpha^2\cos^2\varphi}\left[\left(\frac{\partial\psi'}{\partial\lambda}\right)^2 - \psi'\frac{\partial^2\psi'}{\partial\lambda^2}\right] + \frac{V}{\alpha^2\cos\varphi}\left[\frac{\partial\psi'}{\partial\lambda}\frac{\partial\psi'}{\partial\varphi} - \psi'\frac{\partial^2\psi'}{\partial\lambda\partial\varphi}\right] \\ \frac{U}{\alpha^2\cos\varphi}\left[\frac{\partial\psi'}{\partial\lambda}\frac{\partial\psi'}{\partial\varphi} - \psi'\frac{\partial^2\psi'}{\partial\lambda\partial\varphi}\right] + \frac{V}{\alpha^2}\left[\left(\frac{\partial\psi'}{\partial\varphi}\right)^2 - \psi'\frac{\partial^2\psi'}{\partial\varphi^2}\right]\end{array}\right\},$$

where $p = (pressure/1{,}000\ hPa)$; the basic flow $\boldsymbol{U} = (U, V)^{\mathrm{T}}$, where U and V are zonal and meridional wind components; α is the radius of Earth; φ and λ are the latitude and longitude, respectively; ψ' is the perturbation stream function.

3 INTERDECADAL VARIABILITY OF EURASIAN SPRING SNOW DECREMENT AND ITS RELATIONSHIP WITH THE ECSP

An EOF analysis is applied to the detrended SSD to explore the interdecadal variability of SSD over Eurasia. The first two EOF modes of SSD are well separated from each other according to North et al. (1982), which explain about 16 and 8% of the total variance, respectively. **Figure 1** shows the results of the second EOF mode (EOF2) of Eurasian SSD. The spatial pattern of EOF2 is characterized as a west-east dipole pattern roughly bounded by the Ural Mountains, with a positive center in Western Siberia (WSI) and a negative center in Eastern Europe (EEU) (**Figure 1A**). The two regions of WSI and EEU can also be collectively referred to as the snowmelt key area (SMKA) in this study. The corresponding principal component of EOF2 (PC2) exhibits significant interannual variability, superimposed on two interdecadal changes (**Figure 1B**), with the dipole pattern changing from positive phase to negative phase near the late-1970s and an opposite situation around the mid-2000s. To quantify the interdecadal variability of Eurasian SSD and its connection with the ECSP, the difference of area-averaged snowmelt between the domains with positive values (50°–65°N, 70°–100°E) and negative values (45°–70°N, 40°–60°E) is firstly calculated, and the corresponding series processed by a 9-years low-pass Lanczos filter is further defined as the spring snowmelt index (SSDI). The SSDI is highly consistent with PC2, with the correlation coefficient being 0.8, indicating that the SSDI can largely represent the interdecadal features of Eurasia SSD in the latest 60 years (1961–2020). Thus, the SSDI is used in subsequent analysis (**Figure 1C**).

Corresponding to the dipole pattern of Eurasian SSD, the related ECSP anomaly regressed by the SSDI (**Figure 2A**) displays a meridional quadrupole pattern, with excessive precipitation over the regions of southern China (SC) and Huang-Huai River (HHR) and deficient precipitation over the middle and lower reaches of the Yangtze River Valley (YRV) and Inner Mongolia-northeastern China (IMNC). This spatial pattern is extremely consistent to the second mode of interdecadal variability of ECSP (Wang and Li, 2019), which reflects the significance of spring snow cover in Eurasia to ECSP. The correlation coefficients of the SSDI with four precipitation indexes (PI_1, PI_2, PI_3, and PI_4) that are calculated by the standardized interdecadal components of the area-averaged rainfall over four quadrangles in **Figure 2A** are −0.43, 0.51, −0.49 and 0.72, respectively. To quantify the temporal variability of the quadrupole pattern above, a new

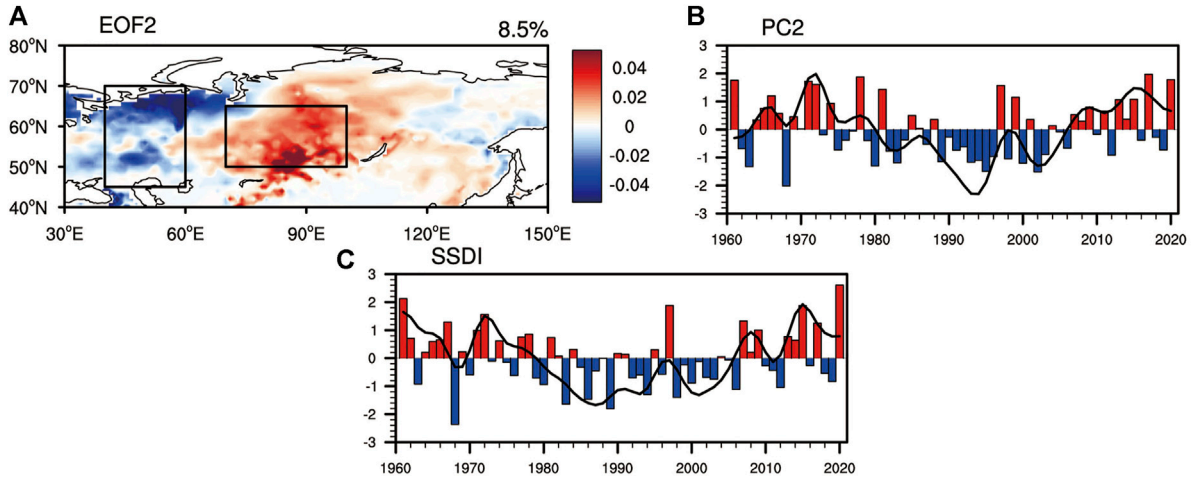

FIGURE 1 | (A) Spatial pattern of the second mode of empirical orthogonal function (EOF2) and **(B)** the corresponding standardized time series of the second principal component (PC2) of Eurasian SSD during 1961–2020. **(C)** Same as **(B)**, but for the difference of SSD between the rectangles with positive values (50°–65°N, 70°–100°E) and negative values (45°–70°N, 40°–60°E). The black lines denote the corresponding 9-years low-pass filtered series.

precipitation index (PI) is defined by the standardized differences between positive values (PI_2, PI_4) and negative values (P1_1, PI_3) (**Figure 2B**). Obviously, the spatial pattern of ECSP relevant to SSDI displays similar interdecadal variation to the SSD, and their correlation coefficient is as high as 0.76. Noted that, the first EOF mode, which mainly reflect the variability of SSD over Northern Eurasia (**Supplementary Figure S1**), show highly weak relationship with ECSP (**Supplementary Figure S2**). Therefore, this study mainly focuses on the second EOF mode of SSD.

The above analysis reveals an evidently close relationship between the Eurasian spring snowmelt over SMKA and the ESCP on interdecadal time scales. However, how is this cross-seasonal teleconnection structure between Eurasian SSD and the ECSP founded? The possible mechanisms will be discussed in the next section.

4 POSSIBLE PHYSICAL MECHANISMS

As is known that soil moisture (SM) plays an important role in the climate system. It can influence the land surface hydrological cycle and energy balance through surface energy partitioning between latent and sensible heat fluxes (Barnett et al., 1989; Cohen and Rind, 1991; Yasunari et al., 1991; Seneviratne et al., 2010; Halder and Drimeyer, 2017). **Figure 3A** shows the SM anomalies regressed onto the SSDI in the shallow layer (0–7 cm) during late spring (May). Corresponding to the west-east dipole pattern of Eurasian SSD (**Figure 1A**), the SM anomalies present homologous features with drier soil in the western region and wetter soil in the eastern region. This correspondence between SSD and SM may be a manifestation of hydrological effect of snow: Increased spring snowmelt (SSD) can produce more water penetrating into the soil, leading to anomalously moist soil and vice versa (Souma and Wang, 2010; Ye and Lau 2019). However, since the nonsynchronous changes of SSD and SM, the regressed significant SM anomalies may exist outside SMKA (**Figure 3A**) and such similar phenomena have also been reported in other researches (Zhang et al., 2017; Sun et al., 2021). Overall, this kind of characteristics corresponds well with the distribution of SSD despite some exceptions, such as areas around Mongolia (**Supplementary Figure S3**). Furthermore, we also found that there is a significant negative center of regressed SM anomalies over Mongolia, but the local spring snow decrement is relatively low (**Supplementary Figure S3A**). Nevertheless, a significant relationship between variability of SSD over SMKA and SM over Mongolia (SMI) is evident on interdecadal scales and the correlation coefficient reaches −0.75. The spring snowmelt anomalies regressed onto SSDI (**Supplementary Figure S3A**) correspond well with that onto SMI (**Supplementary Figure S3B**), suggesting the possible impact of the preceding spring snowmelt over SMKA on late spring (May) SM over Mongolia. For further explanation of the influence way, a detailed investigation on land surface process during snowmelt is needed, which is not included in this paper. In summer (**Figure 3B**), as the snow over Eurasia is nearly melting except in a few areas north of 65°N (figure omitted), sporadic positive values appear at high latitudes, and the positive center of anomalous SM also shifts northward. In particular, there are positive SM anomalies north of 65°N over the EEU, which could be explained by more melting snow in summer related to the below-normal spring snowmelt. Nevertheless, the spatial pattern of SM (0–7 cm) anomaly in summer is highly consistent with that in late spring and the deeper soil layers display coherent features but with relatively larger values (**Supplementary Figure S4**, 100–289 cm). This indicates the SM anomaly caused by snowmelt over the SMKA can persist into the subsequent summer, which has been confirmed in various researches (Xu and Dirmeyer, 2013; Chen S et al., 2016; Chen W et al., 2016; Zhang et al., 2017; Sun et al., 2021). Some studies also argued the

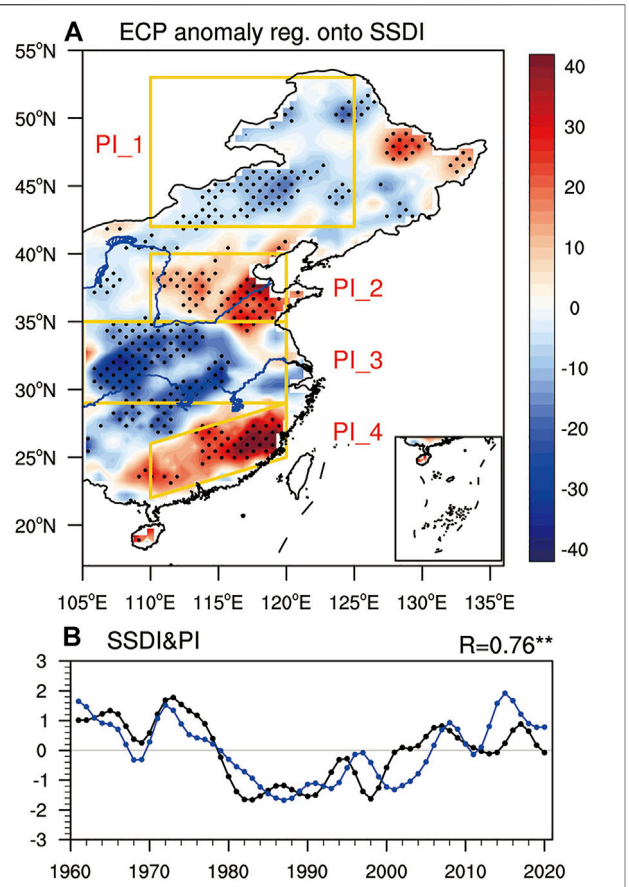

FIGURE 2 | (A) Eastern China precipitation anomaly in summer (JJA) regressed onto the SSDI. **(B)** shows the SSDI (blue line) and Precipitation index (PI, black line), where PI is defined as the differences of rainfall between the standardized interdecadal component over the quadrangles with positive values (PI_2, PI_4) and negative values (PI_1, PI_3) shown in **(A)**. The stippling in **(B)** denotes the regression coefficients statistically significant at the 95% confidence level. *R* in **(B)** represents the correlation coefficients between SSDI and PI, where ** indicates the values passing the significance test at 99% confidence level.

inability of the persistence of snowmelt-induced SM into summer (Robock et al., 2003; Ye and Lau, 2019), which may be related to varying land surface datasets.

The SM in summer can affect land surface thermal balance, and further changes the diabatic heating that affects the atmosphere above (Seneviratne et al., 2010). Regressions of the anomalous surface latent heat flux (**Figure 4A**) and sensible heat flux (**Figure 4B**) onto the SSDI are calculated to analyze the effect of SM on surface thermal conditions in summer. From **Figure 3B** and **Figure 4**, we can find positive (negative) correlations between SM and latent heat flux (sensible heat flux) over the SMKA, especially over the WSI. It could be illustrated as follows: wetter soil with more evaporation can lead to positive latent heat flux transporting from surface to atmosphere, and thus decrease the surface temperature following less upward sensible heat flux, and vice versa. Note that discrepancy between surface latent flux (**Figure 4A**) and SM (**Figure 3B**) in summer is observed over the northern part of EEU and other areas at high latitudes and the possible reason is as follows: Surface latent flux is directly proportional to evapotranspiration, but the dependency of evapotranspiration on SM is influenced by many factors such as precipitation and runoff (Seneviratne et al., 2010), which reflect the complicated process of land surface water cycle.

To elucidate the lagged effect of Eurasian spring snowmelt on local atmospheric circulation in subsequent summer, the spatial distributions of geopotential height and horizontal wind in the upper, middle and lower troposphere regressed onto the SSDI are displayed in **Figure 5**. At the lower troposphere, there are multiple geopotential height anomaly centers lining up from west to east with positive (negative) values appearing near the EEU (WSI), corresponding to the areas with excessive (deficient) spring snowmelt, which is commonly known as the mid-latitude zonal wave train (**Figure 5C**). Similar features can be identified in the upper (**Figure 5A**) and middle (**Figure 5B**) troposphere as well. Above all, the snowmelt-related atmospheric circulation anomalies appear as middle-to-high latitude zonally oriented wave trains with a quasi-barotropic structure. It can be found that the distribution of atmospheric circulation anomalies over SMKA correspond well to that of local surface sensible heat flux anomaly, but have a little difference with surface latent flux anomaly over the EEU. Obviously, significant positive (negative) geopotential height anomalies over the EEU (WSI) in the lower layers (e.g., 850 hPa) can probably be explained by the anomalous warming (cooling) effect of the land surface on the atmosphere above (Sun et al., 2021), which is composed of two heating forms: latent heat flux and sensible heat flux. The anomalous Evaporation Fraction (EF), defined as ratio of latent heat flux to effective energy (Seneviratne et al., 2010) regressed onto SSDI is calculated to specific the proportion of these two heating forms (**Figure 4C**). The results indicate that warming (cooling) effect of the land surface on atmosphere above is mainly realized through the sensible (latent) heating over EEU (WSI), which may explain the similar or different distribution features between **Figure 5** and **Figures 4A,B** respectively.

To further investigate how the atmosphere circulation anomalies develop to the upper troposphere and ultimately appear as a quasi-barotropic structure, the anomalous precipitation and vertical velocity in summer regressed onto the SSDI are calculated (**Figure 6**). Evidently, increased (decreased) precipitation along with whole-layer ascending (descending) flow in the troposphere are found over the negative (positive) center near the WSI (EEU). Dirmeyer et al. (2014) indicated that changes of SM could affect the near-surface atmospheric conditions and may increase or decrease the possibilities of triggering moist convection through affecting the water or energy cycles. Low-level moisture originating from wet soil over the WSI can be lifted to the high level along with the ascending flow against the background of *in-situ* lower-level cyclonic circulation, finally leading to the formation of precipitation. Meanwhile, the latent heat released from this process could also promote the development of cyclonic circulation (Zhang et al., 2003), and thus the lower-level thermal forcing and the middle-to-upper-level circulation anomalies are

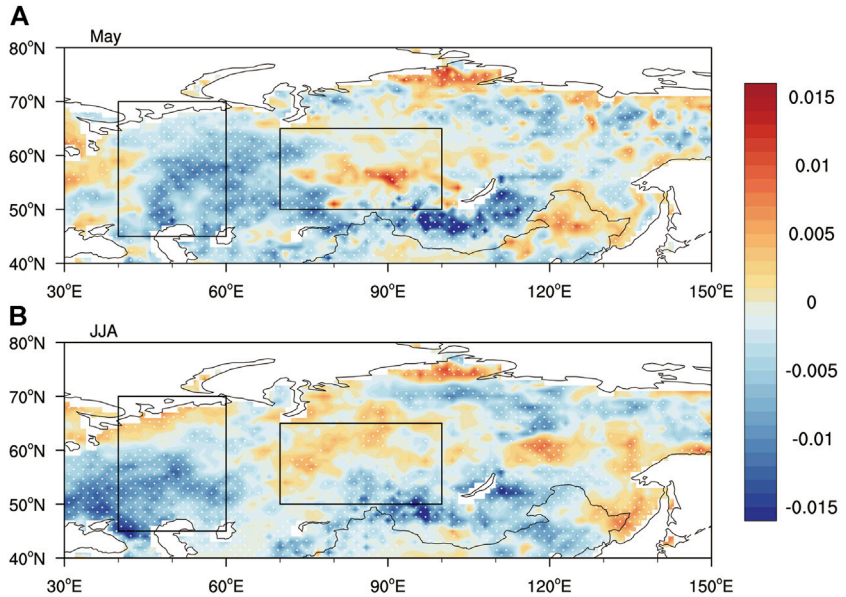

FIGURE 3 | (A) May and **(B)** summer (JJA) 0–7-cm soil moisture anomalies ($m^3\ m^{-3}$) regressed onto the SSDI. The black rectangles are the same as in **Figure 1A**, and the stippling indicates the regression coefficients statistically significant at the 95% confidence level.

linked. The same principle also applies to the development of the anticyclonic circulation over the left of the EEU.

Rossby wave developed upstream could influence or generate the anomalous circulation systems downstream, which is generally called the upstream effect (Li et al., 2020). **Figure 7** depicts the stream function and wave activity flux (WAF) regressed onto the SSDI at 300 hPa in summer. Obviously, there are relatively weak Rossby wave trains in the upper troposphere propagating eastward from the Western Europe, which is reinforced twice over the EEU and WSI and propagate downstream to the Lake Baikal and its vicinity. The WAFs at 500 hPa also display similar characteristics (**Supplementary Figure S5**). The growth of WAFs over two framed areas may be due to the anomalous geopotential height generated from surface thermal forcing, which is associated with the *in-situ* spring snowmelt anomaly. The eastward propagation of wave train could bring the energy generated from spring snowmelt anomalies to downstream areas, and thus cause the positive geopotential height anomaly around the Lake Baikal. It should be noted that the eastward-propagating WAFs over the Lake Baikal are also observed, which split into two branches in the upper troposphere, where one continues to spread eastward and the other weaker branch shifts southward, leading to the negative phase over southern China. Therefore, the linkage between spring SMKA and Eastern-Asia summer circulation can be found.

Additionally, it should be pointed out that the quasi-barotropic anticyclonic circulation existing near the Lake Baikal, the right side of the spring SMKA of this study, could be explained by *in-situ* surface heating (**Figure 4**) as well, which could be explained by local persistent snowmelt-related SM anomalies (**Figure 3B**). Hong et al. (2017) also indicated that northeastern Eurasia is the region of Eurasian surface warming. To confirm this inference, we further do partial correlation of SSDI with 200-, 500-, 850-hPa winds and geopotential heights in summer, in which the parts linearly related to the SM averaged over Mongolia in May are removed (**Figure 8**). The results show that the anticyclonic over Baikal is also observed but weakened. Therefore, we hold that the spring snowmelt over SMKA can influence the downstream atmospheric circulation through the delayed hydrological effect in two combined different ways: the upstream effect and the direct response of atmospheric circulation to local SM anomalies. Above all, the SM anomalies generated from Eurasian spring snowmelt over the EEU and the WSI facilitate the foundation of the quasi-barotropic structure of atmospheric circulation above through the land surface thermal forcing, with a positive center near the EEU and a negative center near the WSI. These geopotential height anomalies upstream further cause the upper-level significant (insignificant) positive (negative) geopotential height anomalies over the regions of Lake Baikal and northern China (southern China). Meanwhile, the surface heating induced by local SM anomalies around Mongolia play a role as well. But how the quadrupole rainfall pattern shown in **Figure 2A** is established under the near dipole pattern of atmospheric circulation over Eastern China related to spring snowmelt needs further investigation.

A detailed check of the anomalous atmospheric circulation and the associated dynamic processes over Eastern China is carried out to investigate the favorable conditions for the occurrences of precipitation patterns related to the SSDI on interdecadal time scales over Eastern China (as shown in **Figure 2A**). Corresponding to the positive SSDI, significant anticyclonic circulation anomalies occupy the northern part of China at 200 hPa, with its center

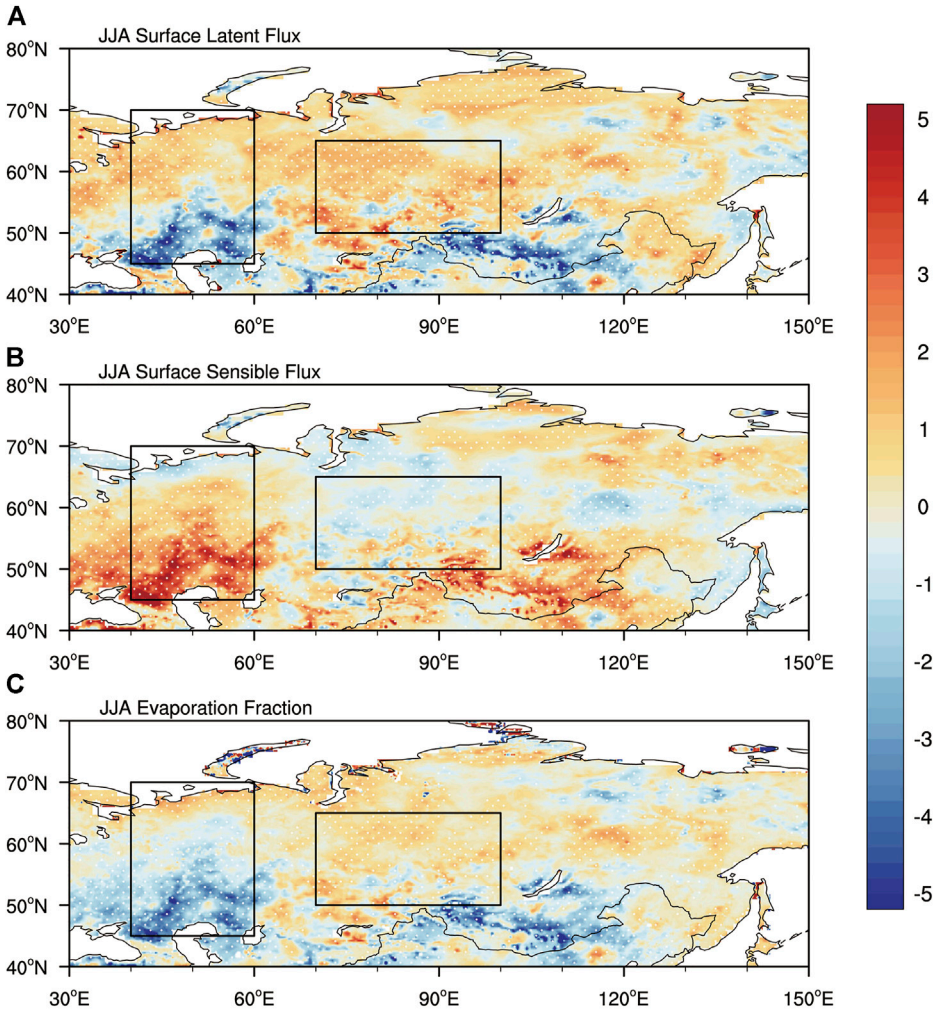

FIGURE 4 | Summer (JJA) **(A)** surface latent flux, **(B)** surface sensible flux anomalies (W m^{-2}) and **(C)** evaporation fraction (%) regressed onto the SSDI. The black rectangles are the same as in **Figure 1A**, and the stippling indicates the regression coefficients statistically significant at the 95% confidence level.

located over south of the Lake Baikal, accompanied by weak cyclonic circulation anomalies occurring over the southern part of China (**Figure 9A**). Similarly, the homologous characteristic is also observed in the middle troposphere, except the positive center slightly titling northward with height (**Figure 9B**), which could be explained by a more zonally oriented propagation of WAFs in the middle troposphere (**Supplementary Figure S5**). Previous studies have proposed and confirmed that the subtropical jet indicates the position of the Eastern Asian summer rain band (Liang and Wang, 1998; Liao et al., 2004; Du et al., 2009). Meanwhile, the subtropical westerly jet can also act as a waveguide in the upper troposphere, thus linking the midlatitude Rossby waves with the East Asian atmospheric circulation systems (Hong and Lu, 2016; Zhang et al., 2017; Han et al., 2021). Therefore, the 200-hPa *V* wind anomaly and the climatological westerly jet are also presented (**Figure 9A**). Obviously, anomalous northerly winds are observed on the right side of this strong anticyclonic circulation system, which is the climatological position of the upper-level jet entrance, with its center over northeastern China. On the right side of the exit region of the upper-level jet, northerly wind components are decreased, the easterly or southeasterly wind predominates, and thus an anomalous convergence of meridional winds appears over the Yangtze River-Korean Peninsula (Brill et al., 1985). As a result, an anomalous upper-level convergence belt and the related convergent winds are observed over the YRV (**Figure 10A**). Based on the principle of mass conservation, the abnormal convergent airflow accumulates in the upper troposphere over the Yangtze River Basin and then sinks, resulting in descending motions at 500 hPa (**Figure 10B**) and the corresponding local divergence in the lower troposphere (**Figure 10C**). Similarly, a strong upper-level divergence of meridional winds with divergent southerly winds is observed over northern China, that is, the left side of the jet exit region, which could give rise to the compensatory lower-level convergence and the cyclonic circulation center over

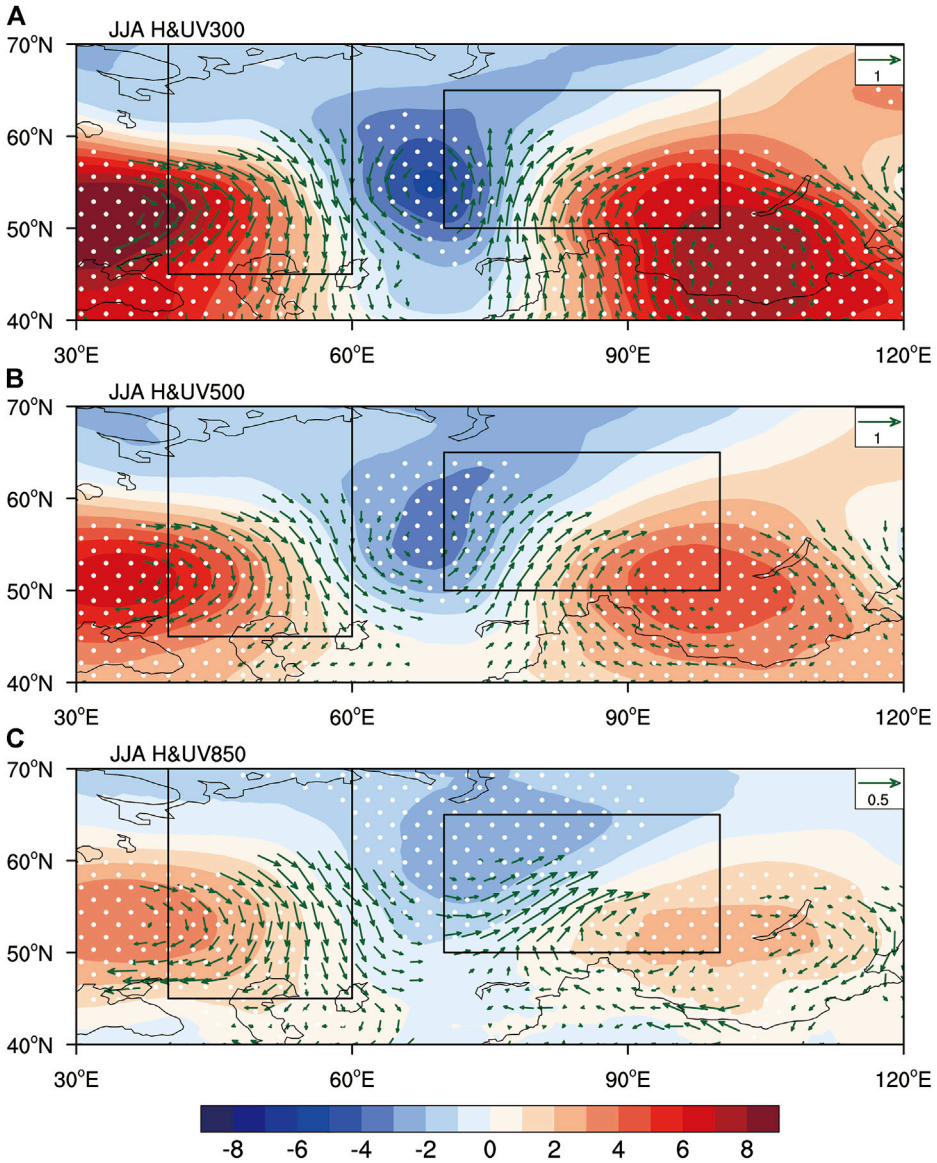

FIGURE 5 | (A) 300-hPa, **(B)** 500-hPa and **(C)** 850-hPa geopotential height anomalies (shading; gpm) and horizontal wind (vectors; m s^{-1}) in summer (JJA) regressed onto SSDI. The black rectangles are the same as **Figure 1A**. The vectors represent the wind statistically significant at the 95% confidence level. The stippling denotes the regression coefficients statistically significant at the 95% confidence level.

the HHR (**Figure 10D**). Therefore, with the coordination of upper-level convergence and lower-level divergence, which could be attributed to the strong anticyclonic circulation anomalies near the Lake Baikal, a uniform descending motion is founded over the YRV and an ascending motion over the HHR. Meanwhile, under the direct control of a middle-to-upper-level high (low) pressure system, anomalous descending (ascending) motion is founded over the IMNC (SC) as well.

For further confirmation, the latitude-pressure cross-section of vertical velocity and meridional wind components regressed onto the SSDI is displayed in **Figure 11A**. Four ascending/descending airflows and the formed meridional circulation are found over Eastern China and commendably correspond to the quadrupole distribution of ECSP, which is consistent with the above results. Above all, under the background of mid- and upper-level atmospheric circulation anomalies, which are characterized as dipole patterns, a quadrupole pattern of secondary circulation shown in **Figure 11A** can be found through the lower-level/upper-level convergent/divergent activities and the related ascending/descending motions. Additionally, to investigate the water vapor conditions, the

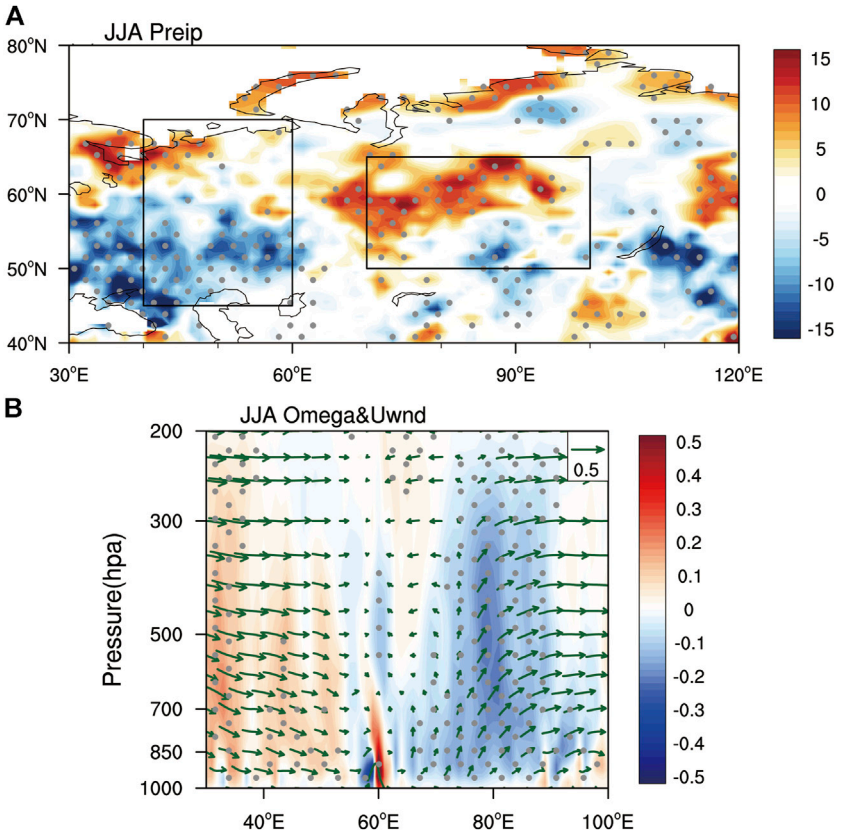

FIGURE 6 | Summer (JJA) **(A)** precipitation (mm) and **(B)** longitude-pressure cross-section of vertical velocity (Pa s^{-1}) averaged along 55°–65°N regressed onto the SSDI. The black rectangles in **(A)** are the same as **Figure 1A**, and the stippling denotes the regression coefficients statistically significant at the 95% confidence level.

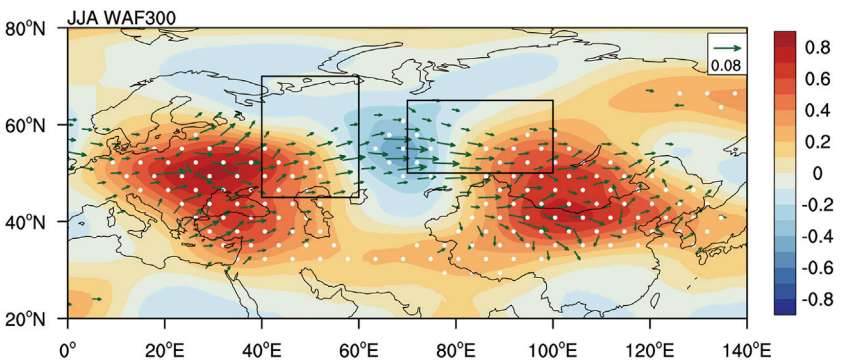

FIGURE 7 | Anomalies of 300-hPa stream function (shading; m2 s−1) and the associated wave activity flux (vectors; m2 s−2) regressed onto the SSDI during summer (JJA). The black rectangles are the same as **Figure 1A**, and the stippling denotes the regression coefficients statistically significant at the 95% confidence level.

regression results of the water vapor transport vertically integrated from surface to 300 hPa and its divergence are also presented in **Figure 11B**. Corresponding to positive SSDI, there are two water vapor transport channels. One is the easterly airflow near the Bohai Sea that transports the water vapor from the Bohai Sea to the HHR and its vicinity, thus inducing distinctive moisture convergence anomalies. While the other is the southeasterly currents that carry water vapor from the northwest Pacific, leading to the anomalous moisture convergence over the SC. Apparently, these moisture conditions and the vertical motions shown in **Figure 11A** favor the rainfall over the regions of HHR and SC and the surroundings, but suppress the occurrence of rainfall over other two areas of Eastern China.

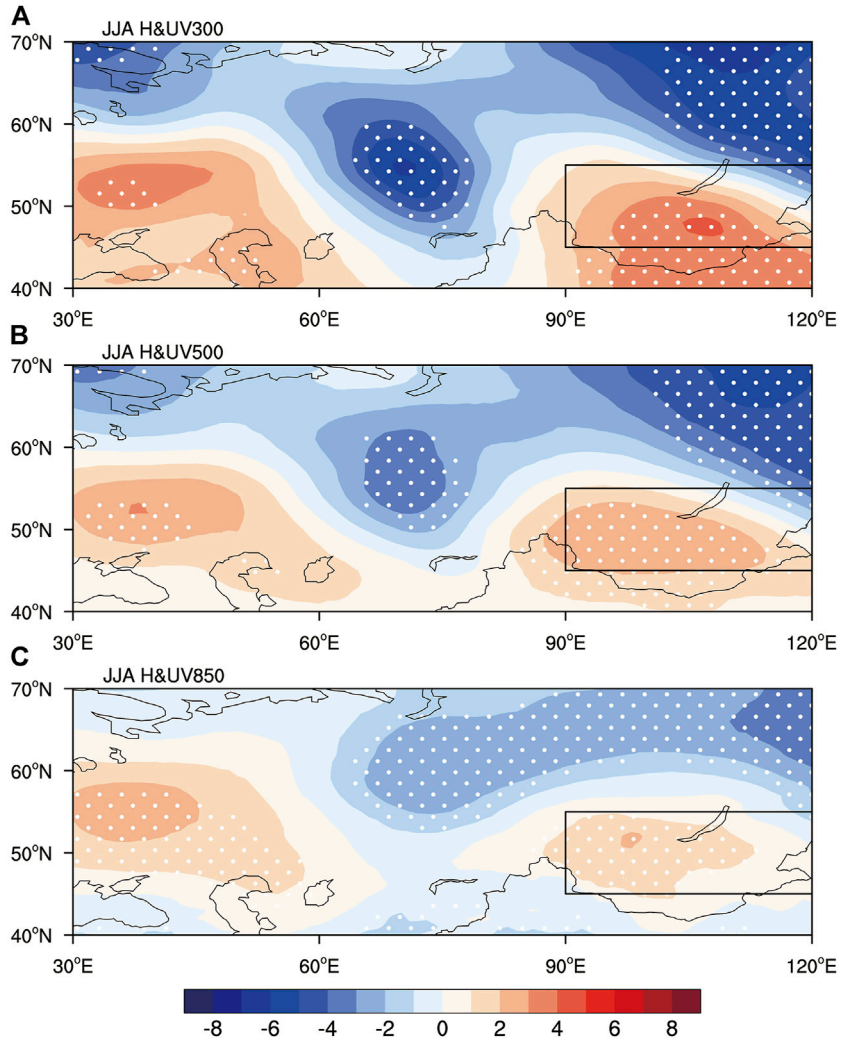

FIGURE 8 | (A) 300-hPa, **(B)** 500-hPa and **(C)** 850-hPa geopotential height anomalies (gpm) in summer (JJA) regressed onto SSDI after removing effect of May soil moisture anomaly over Mongolia (black rectangles: 45°–55°N, 90°–120°E). The stippling denotes the regression coefficients statistically significant at the 95% confidence level.

5 SUMMARY AND DISCUSSION

Based on the ERA5 SWE data and the CMA precipitation data, we explore the interdecadal variability of the Eurasian Spring snowmelt and its impact on the ECSP. The involved mechanisms are also discussed by using the ERA5 land data and other atmospheric data. The results show that the second EOF mode of Eurasian SSD exhibits a west-east dipole pattern, with a negative center located over the EEU and a positive center over the area around WSI. The corresponding principal component of EOF2 (PC2) exhibits significant interannual variability superimposed on two interdecadal changes in the late-1970s and mid-2000s. The anomalous west-east dipole pattern of spring snowmelt is significantly related to the north-south quadrupole pattern of ECSP. With above (below)-normal snowmelt over the WSI (EEU), excessive rainfall over the regions of SC and HHR and deficient precipitation over the regions of YRV and IMNC are observed. The correlation coefficient between SSDI and PI is 0.76, passing the significance test at the 99% confidence level. The anomalous Eurasian Spring snowmelt can induce an anomalous wave train over middle latitudes and enhance the anticyclonic (cyclonic) circulation near the Lake Baikal (southern China), which influences the meridional circulation over Eastern China through the lower-level/upper-level convergent/divergent activities, thus affecting the ECSP.

The detailed processes are as follows. The increased snowmelt over the WSI produces above-normal local SM and persists to the subsequent summer, thereby changing the land surface thermal conditions with more latent flux and less sensible flux transporting to the atmosphere above, ultimately causing anomalously negative anomalies of geopotential height in the low troposphere. Low level moisture generated from wet soil over the WSI can be lifted to the high level along with the ascending

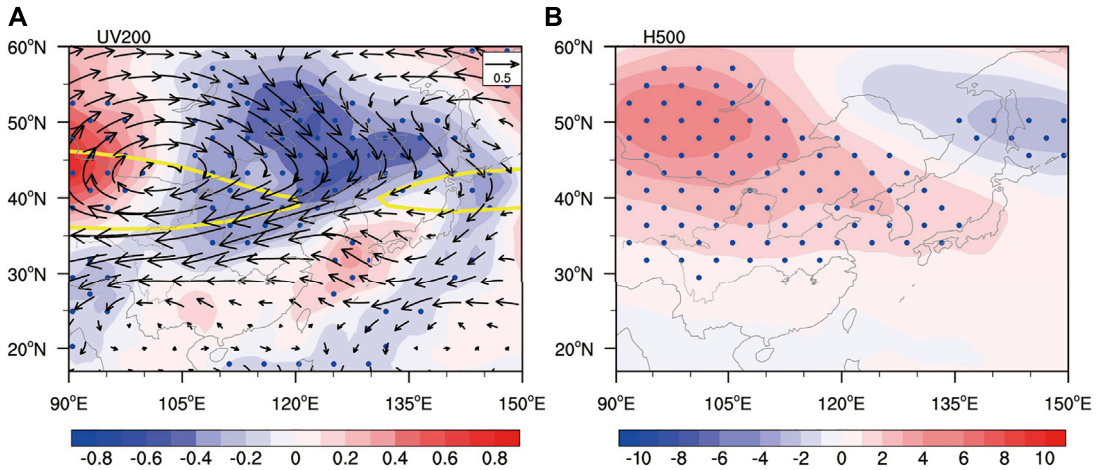

FIGURE 9 | Regression maps of the 9-years low-pass filtered circulations in summer (JJA) concerning the SSDI. **(A)** 200-hPa wind (vector; m s^{-1}) and V wind (shading; m s^{-1}), **(B)** 500-hPa geopotential height (gpm). The stippling denotes the regression coefficients statistically significant at the 95% confidence level. The yellow solid lines in **(A)** indicate the climatological *U* wind of 25 m s^{-1}.

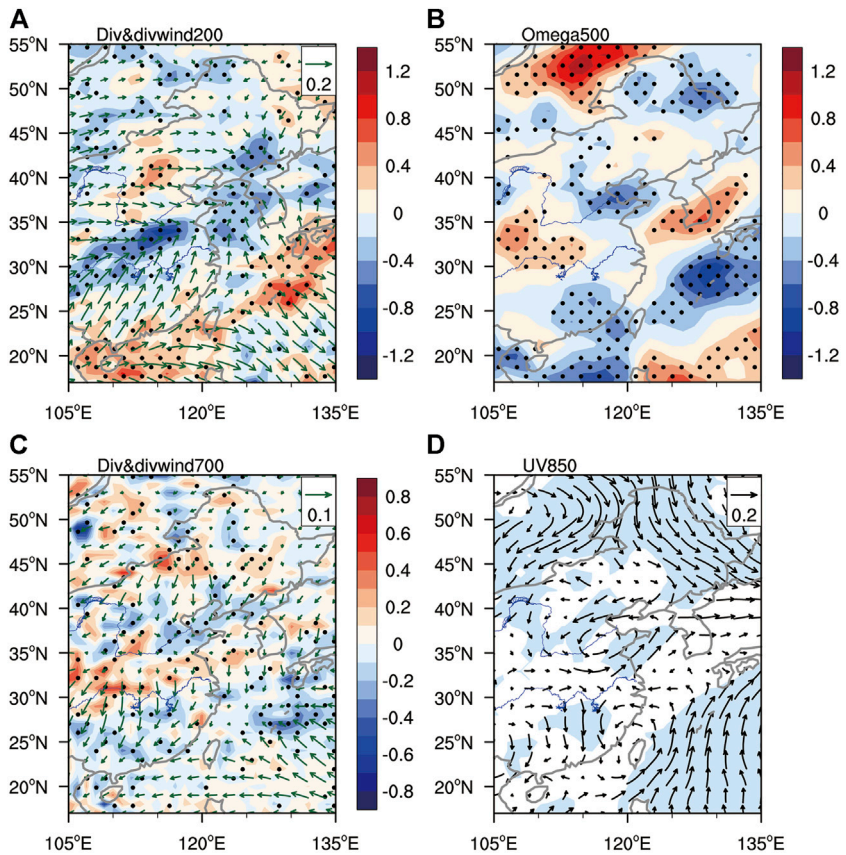

FIGURE 10 | Regression maps of the 9-years low-pass filtered circulations in summer (JJA) with regard to the SSDI. **(A)** 200-hPa divergence (shading; 10^{-6} s^{-1}) and divergent wind (vector; m s^{-1}), **(B)** 500-hPa vertical velocity (10^{-2} Pa s^{-1}), **(C)** same as **(A)**, but for 700 hPa, and **(D)** 850-hPa wind (m s^{-1}). The stippled areas in **(A–C)** and the shaded areas in **(D)** denote the regression coefficients that are statistically significant at the 95% confidence level.

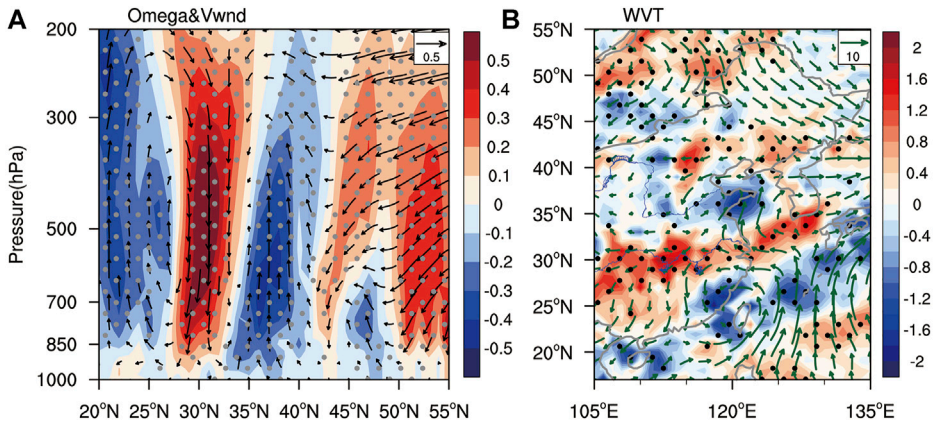

FIGURE 11 | Regression maps of the 9-years low-pass filtered circulations in summer (JJA) with regard to the SSDI. **(A)** The pressure-latitude cross-section of meridional velocity (vector; m s^{-1}) and vertical velocity (shading; 10^{-2} Pa s^{-1}) averaged along 110°–120°E. **(B)** water vapor transport (vector; 100 kg m^{-1} s^{-1}) vertically integrated from surface to 300 hPa and its divergence (shading; $10e^{-7}$ kg m^{-2} s^{-1} hPa^{-1}). The stippling denotes the regression coefficients statistically significant at the 95% confidence level.

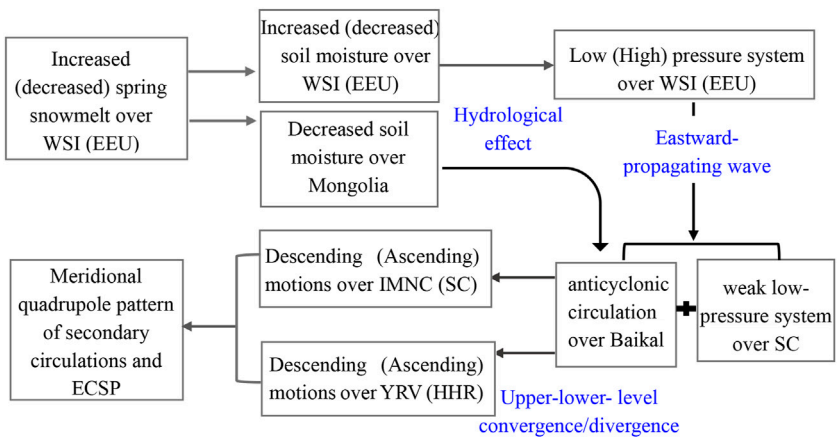

FIGURE 12 | Schematic of the process in which Eurasian spring snowmelt affects Eastern China summer precipitation.

flow related to the *in-situ* lower-level cyclonic circulation, finally resulting in the formation of precipitation. The latent heat of condensation released in the process conversely promotes the development of the cyclonic circulation, thus linking the lower-level thermal forcing and the lower-to-upper-level circulation anomalies. Similarly, the decreased snowmelt over the EEU can also induce positive geopotential height anomalies in the whole troposphere. In terms of the wave propagation, there are eastward WAFs between the middle and upper troposphere, which are strengthened over the EEU and WSI and continue to propagate downstream, thus generating significant anticyclonic circulation anomalies over Baikal and insignificant anticyclonic circulation anomalies over the SC. This may explain the descending (ascending) motion over the IMNC (SC). Noted that, the surface heating around Mongolia, which could be attributed to local snowmelt-over-SMKA-related SM anomalies, can also explain the anomalous anticyclonic over Baikal as well. Subsequently, the reasons for the formation of the quadrupole pattern of the ECSP are discussed. With the amplified anticyclonic circulation near the Lake Baikal and the related anomalous convergence (divergence) of meridional winds, strong upper-level convergence (divergence) belt appears over the YRV (HHR), which is the right (left) side of the exit region of the climatological westerly jet. This leads to the response of middle-to-lower-level atmospheric circulation and the uniform descending (ascending) motions over the YRV (HHR). Therefore, a secondary circulation with a quadrupole pattern is found through the collocation of upper-lower level convergence/divergence and the associated ascending/descending motions. Finally, under favorable conditions of water vapor transport, excessive summer rainfall over the region of HHR and SC and the opposite situation over the regions of IMNC and YRV are observed (**Figure 2A**). The processes of Eurasian spring

snowmelt affecting Eastern China summer precipitation are shown in **Figure 12**.

This study gives a better understanding of the cross-seasonal relationship between the ECSP and the Eurasian snow cover. However, Shen et al. (2020) also implied the role of SST on interannual time scale when investigating the linkage between spring snow cover and ESCP, but how about that on interdecadal time scales. Meanwhile, the possible physical mechanisms from the perspective of hydrological effect of snow cover are also discussed, which could give some reference to the explanation of snow-hydrological effect. Results show that with increased (decreased) spring snowmelt, SM anomalies are formed and can keep the snow cover effects to summer, thus affecting summer atmospheric circulation, which confirms the ability of persistence of snowmelt-induced SM to summer. The connection between snowmelt and SM is a manifestation of the snow-hydrological effect to some extent (Sun et al., 2021). The regressed SM anomalies onto SSDI is displayed in **Figure 3**, indicating the impact of spring snowmelt on SM in late spring (May) and summer. Besides, the TCC (temporal correlation coefficient) between SSDI and SMI on interdecadal time scales, defined the same as SSDI but for SM in late spring, was calculated as well. The TCC is 0.5, exceeding the 99% confidence level, suggesting that spring snowmelt could roughly explain 25% of the total variance of SM anomalies. Nevertheless, there are still some problems to be solved. Although the impact of spring snowmelt to the following SM is discussed by using regression analysis, the quantitative contributions of snowmelt or snowmelt-related infiltration to SM is not clear. In light of Souma and Wang (2010), further exploration with the aid of sensitive simulations is required to deal with such issue.

Besides, the following points are worthy of further explanation as well. First, the conclusions above are maintained based on JRA55 datasets as well (**Supplementary Figures S6, S7, S8**), indicating the robust conclusions that are not sensitive to the use of datasets. Second, although previous studies demonstrate the significant albedo effect of snow cover (Yasunari et al., 1991; Souma and Wang, 2010), this study mainly discusses the hydrological effects related to spring snowmelt considering that the albedo effect of snow cover mainly works before or during the snow melting process (Xu and Dirmeyer, 2013; Halder and Dirmeyer, 2017) and the snow over of the key area we studied has melted in summer. As such, the snowmelt-related soil moisture anomaly is focused in this study. In addition, there is a strong interaction between snowmelt and the atmosphere in spring (Xu and Dirmeyer, 2013), which is not discussed in this study, and how much the snow cover contributes to the anomalous circulation related to the ECSP requires further diagnostic analysis. Above all, the related dynamical mechanisms explaining the relationship between Eurasian spring snowmelt and ECSP still need further investigation.

DATA AVAILABILITY STATEMENT

The original contributions presented in the study are included in the article/**Supplementary Material**, further inquiries can be directed to the corresponding author.

AUTHOR CONTRIBUTIONS

FC: Conceptualization, Data curation, Formal analysis, Methodology, Software, Visualization, Writing—original draft. QL: Conceptualization, Funding acquisition, Methodology, Supervision, Writing—review and editing. JW: Methodology, Writing—review and editing. YL: Conceptualization, Writing—review and editing. YD:Writing—review and editing XS:Writing—review and editing. CS: Data curation.

FUNDING

This work was supported by the Strategic Priority Research Program of Chinese Academy of Sciences (Grant No. XDA20100304), the Second Tibetan Plateau Scientific Expedition and Research (STEP) program (Grant No. 2019QZKK0102 and 2019QZKK0208), the National Natural Science Foundation of China (Grant No. 41790471), and National Key R & D Program of China (Grant No. 2018YFC1505806).

SUPPLEMENTARY MATERIAL

The Supplementary Material for this article can be found online at: https://www.frontiersin.org/articles/10.3389/feart.2022.927876/full#supplementary-material

REFERENCES

Barnett, T. P., Dümenil, L., Schlese, U., Roeckner, E., and Latif, M. (1989). The Effect of Eurasian Snow Cover on Regional and Global Climate Variations. *J. Atmos. Sci.* 46 (5), 661–686. doi:10.1175/1520-0469(1989)046<0661:TEOESC>2.0.CO;2

Bell, B., Hersbach, H., Simmons, A., Berrisford, P., Dahlgren, P., Horányi, A., et al. (2021). The ERA5 Global Reanalysis: Preliminary Extension to 1950. *Quart. J. R. Meteoro Soc.* 147 (741), 4186–4227. doi:10.1002/qj.4174

Brill, K. F., Uccellini, L. W., Burkhart, R. P., Warner, T. T., and Anthes, R. A. (1985). Numerical Simulations of a Transverse Indirect Circulation and Low-Level Jet in the Exit Region of an Upper-Level Jet. *J. Atmos. Sci.* 42 (12), 1306–1320. doi:10.1175/1520-0469(1985)042<1306:NSOATI>2.0.CO;2

Chen, S., Wu, R., and Liu, Y. (2016). Dominant Modes of Interannual Variability in Eurasian Surface Air Temperature during Boreal Spring. *J. Clim.* 29 (3), 1109–1125. doi:10.1175/JCLI-D-15-0524.1

Chen, W., Hong, X., Lu, R., Jin, A., Jin, S., Nam, J.-C., et al. (2016). Variation in Summer Surface Air Temperature over Northeast Asia and its Associated Circulation Anomalies. *Adv. Atmos. Sci.* 33 (1), 1–9. doi:10.1007/s00376-015-5056-0

Chen, X. F., and Song, W. L. (2000). Analysis of Relationship between Snow Cover on Eurasia and Tibetan Plateau in Winter and Summer Rainfall in China and Application to Prediction. *Plateau. Meteor.* 19 (5), 216–223. (in chinese).

Cohen, J., and Rind, D. (1991). The Effect of Snow Cover on the Climate. *J. Clim.* 4 (7), 689–706. doi:10.1175/1520-0442(1991)004<0689:TEOSCO>2.0.CO;2

Dash, S. K., Singh, G. P., Shekhar, M. S., and Vernekar, A. D. (2005). Response of the Indian Summer Monsoon Circulation and Rainfall to Seasonal Snow Depth Anomaly over Eurasia. *Clim. Dyn.* 24 (1), 1–10. doi:10.1007/s00382-004-0448-3

Ding, Y., Wang, Z., and Sun, Y. (2008). Inter-decadal Variation of the Summer Precipitation in East China and its Association with Decreasing Asian Summer monsoon.Part I: Observed Evidences. *Int. J. Climatol.* 28 (9), 1139–1161. doi:10.1002/joc.1615

Dirmeyer, P. A., Wang, Z., Mbuh, M. J., and Norton, H. E. (2014). Intensified Land Surface Control on Boundary Layer Growth in a Changing Climate. *Geophys. Res. Lett.* 41 (4), 1290–1294. doi:10.1002/2013GL058826

Du, Y., Zhang, Y. C., and Xie, Z. Q. (2009). Location Variation of the East Asia Subtropical Westerly Jet and its Effect on the Summer Precipitation Anomaly over Eastern China. *J. Atmos. Sci.* 33 (3), 581–592. doi:10.3878/j.issn.1006-9895.2009.03.15

Duchon, C. E. (1979). Lanczos Filtering in One and Two Dimensions. *J. Appl. Meteor.* 18 (8), 1016–1022. doi:10.1175/1520-0450(1979)018<1016:LFIOAT>2.0.CO;2

Essery, R. (1997). Seasonal Snow Cover and Climate Change in the Hadley Centre GCM. *Ann. Glaciol.* 25, 362–366. doi:10.3189/S0260305500014282

Gong, G., Entekhabi, D., Cohen, J., and Robinson, D. (2004). Sensitivity of Atmospheric Response to Modeled Snow Anomaly Characteristics. *J. Geophys. Res.* 109 (D6), a–n, doi:10.1029/2003JD004160

Halder, S., and Dirmeyer, P. A. (2017). Relation of Eurasian Snow Cover and Indian Summer Monsoon Rainfall: Importance of the Delayed Hydrological Effect. *J. Clim.* 30 (4), 1273–1289. doi:10.1175/JCLI-D-16-0033.1

Han, D., Chen, H. S., Xu, B., Qi, D., and Wu, B. (2014). Impact of Spring Snowmelt over the Eurasian Continent on Summer Rainfall in Yangtze River Valley. *J. Meteo. Sci.* 34 (3), 237–242. doi:10.3969/2014jms.0015

Han, T., Zhang, M., Zhu, J., Zhou, B., and Li, S. (2021). Impact of Early Spring Sea Ice in Barents Sea on Midsummer Rainfall Distribution at Northeast China. *Clim. Dyn.* 57 (3-4), 1023–1037. doi:10.1007/s00382-021-05754-4

He, C., Lin, A., Gu, D., Li, C., Zheng, B., and Zhou, T. (2017). Interannual Variability of Eastern China Summer Rainfall: the Origins of the Meridional Triple and Dipole Modes. *Clim. Dyn.* 48 (1-2), 683–696. doi:10.1007/s00382-016-3103-x

Hong, X., Lu, R., and Li, S. (2017). Amplified Summer Warming in Europe-West Asia and Northeast Asia after the Mid-1990s. *Environ. Res. Lett.* 12 (9), 094007. doi:10.1088/1748-9326/aa7909

Hong, X., and Lu, R. (2016). The Meridional Displacement of the Summer Asian Jet, Silk Road Pattern, and Tropical SST Anomalies. *J. Clim.* 29 (10), 3753–3766. doi:10.1175/JCLI-D-15-0541.1

Kripalani, R. H., Kim, B.-J., Oh, J.-H., and Moon, S.-E. (2002). Relationship between Soviet Snow and Korean Rainfall. *Int. J. Climatol.* 22 (11), 1313–1325. doi:10.1002/joc.809

Li, D. L., and Wang, C. X. (2011). Research Progress of Snow Cover and its Influence on China Climate. *Trans. Atmos. Sci.* 34 (5), 627–636. doi:10.13878/j.cnki.dqkxxb.2011.05.013

Li, H., He, S., GaoChen, Y. H. P., Chen, H., and Wang, H. (2020). North Atlantic Modulation of Interdecadal Variations in Hot Drought Events over Northeastern China. *J. Clim.* 33 (10), 4315–4332. doi:10.1175/JCLI-D-19-0440.1

Liang, X.-Z., and Wang, W.-C. (1998). Associations between China Monsoon Rainfall and Tropospheric Jets. *Q.J R. Mater. Soc.* 124 (552), 2597–2623. doi:10.1002/qj.49712455204

Liao, G. H., Gao, S. T., Wang, H. J., and Tao, S. Y. (2004). Anomalies of the Extratropical Westerly Jet in the North Hemisphere and Their Impacts on East Asian Summer Monsoon Climate Anomalies. *Chin. J. Geophys.* 47 (1), 10–18. (in Chinese). doi:10.1002/cjg2.449

Liu, X., and Yanai, M. (2002). Influence of Eurasian Spring Snow Cover on Asian Summer Rainfall. *Int. J. Climatol.* 22 (9), 1075–1089. doi:10.1002/joc.784

Lu, M., Kuang, Z., Yang, S., Li, Z., and Fan, H. (2020). A Bridging Role of Winter Snow over Northern China and Southern Mongolia in Linking the East Asian Winter and Summer Monsoons. *J. Clim.* 33 (22), 9849–9862. doi:10.1175/JCLI-D-20-0298.1

Lu, M. M., Wu, R. G., Yang, S., and Wang, Z. B. (2020). Relationship between Eurasian Cold-Season Snows and Asian Summer Monsoons: Regional Characteristics and Seasonality. *Trans. Atmos. Sci.* 43 (1), 93–103. doi:10.13878/j.cnki.dqkxxb.20191025001

North, G. R., Bell, T. L., Cahalan, R. F., and Moeng, F. J. (1982). Sampling Errors in the Estimation of Empirical Orthogonal Functions. *Mon. Wea. Rev.* 110 (7), 699–706. doi:10.1175/1520-0493(1982)110<0699:SEITEO>2.0.CO;2

Pyper, B. J., and Peterman, R. M. (1998). Comparison of Methods to Account for Autocorrelation in Correlation Analyses of Fish Data. *Can. J. Fish. Aquat. Sci.* 55 (9), 2127–2140. doi:10.1139/f98-104

Robinson, D. A., Dewey, K. F., and Heim, R. R. (1993). Global Snow Cover Monitoring: an Update. *Bull. Amer. Meteor. Soc.* 74 (9), 1689–1696. doi:10.1175/1520-0477(1993)074<1689:GSCMAU>2.0.CO;2

Robock, A., Mu, M. Q., Vinnikov, K., and Robinson, D. (2003). Land Surface Conditions over Eurasia and Indian Summer Monsoon Rainfall. *J. Geophys. Res.* 108 (D4), 4131. doi:10.1029/2002JD002286

Seneviratne, S. I., Corti, T., Davin, E. L., Hirschi, M., Jaeger, E. B., Lehner, I., et al. (2010). Investigating Soil Moisture-Climate Interactions in a Changing Climate: a Review. *Earth-Science Rev.* 99 (3-4), 125–161. doi:10.1016/j.earscirev.2010.02.004

Shen, H., Li, F., He, S., Orsolini, Y. J., and Li, J. (2020). Impact of Late Spring Siberian Snow on Summer Rainfall in South-Central China. *Clim. Dyn.* 54 (7-8), 3803–3818. doi:10.1007/s00382-020-05206-5

Souma, K., and Wang, Y. (2010). A Comparison between the Effects of Snow Albedo and Infiltration of Melting Water of Eurasian Snow on East Asian Summer Monsoon Rainfall. *J. Geophys. Res.* 115 (D2), D02115. doi:10.1029/2009JD012189

Sun, B., and Wang, H. (2015). Inter-decadal Transition of the Leading Mode of Inter-annual Variability of Summer Rainfall in East China and its Associated Atmospheric Water Vapor Transport. *Clim. Dyn.* 44 (9-10), 2703–2722. doi:10.1007/s00382-014-2251-0

Sun, Y., Chen, H., Zhu, S., Zhang, J., and Wei, J. (2021). Influence of the Eurasian Spring Snowmelt on Summer Land Surface Warming over Northeast Asia and its Associated Mechanism. *J. Clim.* 34 (12), 1–65. doi:10.1175/JCLI-D-20-0756.1

Takaya, K., and Nakamura, H. (2001). A Formulation of a Phase-independent Wave-Activity Flux for Stationary and Migratory Quasigeostrophic Eddies on a Zonally Varying Basic Flow. *J. Atmos. Sci.* 58 (6), 608–627. doi:10.1175/1520-0469(2001)058<0608:AFOAPI>2.0.CO;2

Wang, H., and Li, D. L. (2019). The Impacts of Global Sea Surface Temperature on Decadal Transitions of Summer Precipitation over Eastern China at Global Warming Transition Points. *J. Trop. Meteor.* 35 (3), 398–408. doi:10.16032/j.issn.1004-4965.2019.037

Wu, B., Yang, K., and Zhang, R. (2009). Eurasian Snow Cover Variability and its Association with Summer Rainfall in China. *Adv. Atmos. Sci.* 26 (1), 31–44. doi:10.1007/s00376-009-0031-2

Wu, R., and Kirtman, B. P. (2007). Observed Relationship of Spring and Summer East Asian Rainfall with Winter and Spring Eurasian Snow. *J. Clim.* 20 (7), 1285–1304. doi:10.1175/JCLI4068.1

Xu, L., and Dirmeyer, P. (2013). Snow-Atmosphere Coupling Strength. Part II: Albedo Effect versus Hydrological Effect. *J. Hydrometeorol.* 14 (2), 404–418. doi:10.1175/JHM-D-11-0103.1

Xu, X., Guo, J., KoikeLiu, T. Y. J., Liu, Y., Shi, X., Zhu, F., et al. (2012). "Downstream Effect" of Winter Snow Cover over the Eastern Tibetan Plateau on Climate Anomalies in East Asia. *J. Meteorological Soc. Jpn.* 90C, 113–130. doi:10.2151/jmsj.2012-C08

Yang, S., and Xu, L. (1994). Linkage between Eurasian Winter Snow Cover and Regional Chinese Summer Rainfall. *Int. J. Climatol.* 14 (7), 739–750. doi:10.1002/joc.3370140704

Yasunari, T., Kitoh, A., and Tokioka, T. (1991). Local and Remote Responses to Excessive Snow Mass over Eurasia Appearing in the Northern Spring and Summer Climate. *J. Meteorological Soc. Jpn.* 69 (4), 473–487. doi:10.2151/jmsj1965.69.4_473

Ye, K., and Lau, N.-C. (2019). Characteristics of Eurasian Snowmelt and its Impacts on the Land Surface and Surface Climate. *Clim. Dyn.* 52 (1-2), 1115–1138. doi:10.1007/s00382-018-4180-9

Yim, S.-Y., Jhun, J.-G., Lu, R., and Wang, B. (2010). Two Distinct Patterns of Spring Eurasian Snow Cover Anomaly and Their Impacts on the East Asian Summer Monsoon. *J. Geophys. Res.* 115 (D22), D22113. doi:10.1029/2010JD013996

Zhang, R. H., Wu, B. Y., Zhao, P., and Han, J. P. (2008). The Decadal Shift of the Summer Climate in Eastern China in Late 1980s and its Possible Causes. *Acta. Meteor. Sin.* 66 (5), 698–706. doi:10.11676/qxxb2008.064

Zhang, R. H., Zhang, R. N., and Zuo, Z. Y. (2016). An Overview of Wintertime Snow Cover Characteristics over China and the Impact of Eurasian Snow Cover on Chinese Climate. *J. Appl. Meteor. Sci.* 27 (5), 513–526. doi:10.11898/1001-7313.20160501

Zhang, R., Zhang, R., and Zuo, Z. (2017). Impact of Eurasian Spring Snow Decrement on East Asian Summer Precipitation. *J. Clim.* 30 (9), 3421–3437. doi:10.1175/JCLI-D-16-0214.1

Zhang, T., Wang, T., Feng, Y., Li, X., and Krinner, G. (2021). An Emerging Impact of Eurasian Spring Snow Cover on Summer Rainfall in Eastern China. *Environ. Res. Lett.* 16 (5), 054012. doi:10.1088/1748-9326/abf688

Zhang, Y. S., Tim, L., and Wang, B. (2003). Decadal Change of the Spring Snow Depth over the Tibetan Plateau: The Associated Circulation and Influence on the East Asian Summer Monsoon. *J. Clim.* 17 (14), 2780–2793. doi:10.1175/1520-0442(2004)017<2780:DCOTSS>2.0.CO;2

Zhang, Z., Sun, X., and Yang, X.-Q. (2018). Understanding the Interdecadal Variability of East Asian Summer Monsoon Precipitation: Joint Influence of Three Oceanic Signals. *J. Clim.* 31 (14), 5485–5506. doi:10.1175/JCLI-D-17-0657.1

Zhou, J., Zuo, Z., and He, Q. (2021). Influence of Eurasian Spring Snowmelt on Surface Air Temperature in Late Spring and Early Summer. *J. Clim.* 34 (20), 1–45. doi:10.1175/JCLI-D-21-0111.1

Conflict of Interest: The authors declare that the research was conducted in the absence of any commercial or financial relationships that could be construed as a potential conflict of interest.